The Hopf bifurcation with bounded noise

Ryan T. Botts[1], Ale Jan Homburg[2,3], and Todd R. Young[4]

[1]Department of Mathematical, Information & Computer Sciences, Point Loma Nazarene University, 3900 Lomaland Drive, CA 92106 San Diego, USA
[2]KdV Institute for Mathematics, University of Amsterdam, Science Park 904, 1098 XH Amsterdam, Netherlands
[3]Department of Mathematics, VU University Amsterdam, De Boelelaan 1081, 1081 HV Amsterdam, Netherlands
[4]Department of Mathematics, Ohio University, 321 Morton Hall, OH 45701 Athens, USA

July 7, 2011

Abstract

We study Hopf-Andronov bifurcations in a class of random differential equations (RDEs) with bounded noise. We observe that when an ordinary differential equation that undergoes a Hopf bifurcation is subjected to bounded noise then the bifurcation that occurs involves a discontinuous change in the Minimal Forward Invariant set.

1 Introduction

We will consider Hopf-Andronov bifurcations in a class of random differential equations (RDEs)

$$\dot{x} = f_\lambda(x) + \varepsilon\xi_t \tag{1}$$

as the parameter $\lambda \in \mathbb{R}$ is varied. Here x will belong to the plane and ξ_t will be a realization of some noise. We are interested in bounded noise in which ξ_t takes values in a closed disk $\Delta \subset \mathbb{R}^2$. More specifically we will consider Hopf-Andronov bifurcations with radially symmetric noise where ξ_t takes values in the unit disk. The RDEs without noise, for $\varepsilon = 0$, unfold a Hopf-Andronov bifurcation as λ varies. We denote by $\mathcal{U}$ the collection of all possible realizations of the noise. We assume that f and $\mathcal{U}$ are sufficiently well-behaved that the equations (1) uniquely defines a flow $\Phi^t(x, \xi)$ for all realizations ξ of the noise.

For the general framework of random dynamical systems we refer the reader to L. Arnold's book [1] (see also [5, 12]). A distinctive feature of dynamical systems with bounded noise is that they may admit more than one stationary measure. For discrete time Markov processes these measures were studied by Doob [7], who showed that their supports are precisely the *minimal forward invariant* (MFI) sets. In [10] the authors adapted Doob's proof to the case of the continuous time (not necessarily Markov) processes generated by RDEs on compact manifolds. It was observed ([10, 15]) that these stationary measures can experience dramatic changes, such as a change in the number of stationary measures or a discontinuous change in one of the supports of densities. We refer to such changes as *hard bifurcations*. Given the one-to-one correspondence between stationary measures and the MFI sets on which they are supported, in order to study hard bifurcations, it is sufficient to study the bifurcations of MFI sets themselves.

We adopt from [11] the following assumptions on (1) and its flow:

H1. The set Δ is a closed disk with smooth boundary. For each x the map $\Delta \to T_xX$ given by $\xi \mapsto f(x,\xi)$ is a diffeomorphism with a strictly convex image $D(x) = f(x,\Delta)$.

H2. There exist $r_0 > 0$ and $t_1 > 0$ such that

$$\Phi_\lambda^t(x,\mathcal{U}) \supset B(\Phi_\lambda^t(x,0), r_0) \qquad \forall t \geq t_1.$$

In [11], under these noise conditions the authors provided a complete classification of bounded noise co-dimension one hard bifurcations in phase space dimensions 1 and 2. We call a set $F \subset X$ *forward invariant* if

$$\Phi_\lambda^t(F,\mathcal{U}) \subset F \tag{2}$$

for all $t \in \mathbb{R}^+$. Denote by $\mathcal{F}$ the collection of forward invariant sets. There is a partial ordering on $\mathcal{F}$ by inclusion, i.e. $E \preceq F$ if $E \subset F$. We call $E \subset \mathcal{F}$ a *minimal forward invariant* (MFI) set if it is minimal with respect to the partial ordering $\preceq$. In this context, MFI sets were shown to exist in [10]. It follows easily from the definitions that an MFI set for (1) is open and connected and that the closures of different MFI are disjoint.

A natural assumption is further that we are given a θ^t-invariant, ergodic probability measure $\mathbb{P}$ on $\mathcal{U}$ with the following hypothesis:

H3. There exist $t_2 > 0$ so that $\Phi_\lambda^t(a)(x)_*\mathbb{P}$ is absolutely continuous w.r.t. a Riemannian measure m on X for all $t > t_2$ and all $x \in X$.

Under this assumption, the closures of MFIs are supports of stationary densities [10]. We note that the concept of MFI set is the same as the concept of *positively invariant maximal control sets* defined in the context of control theory [6]. We now define bifurcation of MFI sets.

Definition 1.1. *A* bifurcation *of MFI sets is said to occur in a parameterized family of random differential equations if either:*

B1 *The number of MFI sets changes.*

B2 *A MFI set changes discontinuously with respect to the Hausdorff metric.*

In a supercritical Hopf bifurcation taking place in (1) for $\varepsilon = 0$, a stable limit cycle appears in the bifurcation at $\lambda = 0$. For a fixed negative value of λ, the differential equations without noise posses a stable equilibrium and the RDE with small noise has an MFI which is a disk around the equilibrium. Likewise, at a fixed positive value of λ for which (1) without noise possesses a stable limit cycle, small noise will give an annulus as MFI. A bifurcation of stationary measures takes place when varying λ. We will prove the following bifurcation scenario for small $\varepsilon > 0$: the RDE (1) undergoes a hard bifurcation of type **B2** in which a globally attracting MFI set changes discontinuously, by suddenly developing a "hole". This hard bifurcation takes place at a delayed parameter value $\lambda = \mathcal{O}(\varepsilon^{2/3})$. We include a brief discussion of attracting random cycles. Finally we demonstrate the results with numerical experiments on a radially symmetric Hopf bifurcation with bounded noise.

For recent studies of Hopf bifurcations in stochastic differential equations (SDEs) we refer to [2–4, 14]. In such systems there is a unique stationary measure, with support equal to the entire state space. Bifurcations of supports of stationary measures, as arising in RDEs with bounded noise, do not arise in the context of SDEs.

2 Random perturbations of a planar Hopf-Andronov bifurcation

Consider a smooth family of planar random differential equations

$$(\dot{x}, \dot{y}) = f_\lambda(x, y) + \varepsilon(u, v) \tag{3}$$

where $\lambda \in \mathbb{R}$ is a parameter and u, v are noise terms from $\Delta = \{u^2 + v^2 \leq 1\}$, representing radially symmetric noise. Hypothesis **H1** is therefore fulfilled, we consider noise such that also **H2** is satisfied.

We assume that without the noise terms, i.e. for $\varepsilon = 0$, the family of differential equations unfolds a supercritical Hopf bifurcation at $\lambda = 0$ [13]. The Hopf bifurcation in planar RDEs with small bounded noise is described in the following result.

Theorem 2.1. *Consider a family of RDEs (3) depending on one parameter λ, that unfolds, when $\varepsilon = 0$, a supercritical Hopf bifurcation at $\lambda = 0$. For small $\varepsilon > 0$ and λ near 0, there is a unique MFI set E_λ. There is a single hard bifurcation at $\lambda_{\text{bif}} = \mathcal{O}(\varepsilon^{2/3})$ as $\varepsilon \downarrow 0$. At $\lambda = \lambda_{\text{bif}}$ the MFI set E_λ changes from a set diffeomorphic to a disk for $\lambda < \lambda_{\text{bif}}$ to a set diffeomorphic to an annulus for $\lambda \geq \lambda_{\text{bif}}$. At λ_{bif} the inner radius of this annulus is $r^* = O(\varepsilon^{1/3})$.*

Proof. We first bring the system without the noise terms,

$$(\dot{x}, \dot{y}) = f_\lambda(x, y), \tag{4}$$

into normal form. Note that a smooth coordinate transformation h_λ and a multiplication by a smooth positive function α_λ (which is equivalent to a time reparameterization), change (4) into

$$(\dot{x}, \dot{y}) = \alpha_\lambda(x, y)(h_\lambda)_* f_\lambda(x, y) = \alpha_\lambda(x, y) Dh(h^{-1}(x, y)) f_\lambda(h^{-1}(x, y)). \tag{5}$$

A smooth normal form transformation consists of a smooth coordinate transformation h_λ, a time reparameterization, and an additional reparametrization of the parameter λ. There exists a smooth normal form transformation that changes (4) into

$$\begin{pmatrix} \dot{x} \\ \dot{y} \end{pmatrix} = \begin{pmatrix} \lambda & -1 \\ 1 & \lambda \end{pmatrix} \begin{pmatrix} x \\ y \end{pmatrix} - r^2 \begin{pmatrix} x \\ y \end{pmatrix} + \mathcal{O}(r^4), \tag{6}$$

see [13] (here $r = \sqrt{x^2 + y^2}$). Applying this normal form transformation to (3) yields

$$\begin{pmatrix} \dot{x} \\ \dot{y} \end{pmatrix} = \begin{pmatrix} \lambda & -1 \\ 1 & \lambda \end{pmatrix} \begin{pmatrix} x \\ y \end{pmatrix} - r^2 \begin{pmatrix} x \\ y \end{pmatrix} + \mathcal{O}(r^4) + \varepsilon A(x, y, \lambda) \begin{pmatrix} u \\ v \end{pmatrix} \tag{7}$$

where $A(x, y, \lambda) = A_0(\lambda) + \mathcal{O}(r)$ is a two by two matrix that depends smoothly on its arguments. Note that expression (5) implies that the noise terms (u, v) are the same as in (3); they only get multiplied by a matrix $A(x, y, \lambda)$. Changing to polar coordinates we find

$$\begin{aligned} \dot{r} &= \lambda r - r^3 + \mathcal{O}(r^4) + \varepsilon \left\langle A \begin{pmatrix} u \\ v \end{pmatrix}, \begin{pmatrix} \cos\theta \\ \sin\theta \end{pmatrix} \right\rangle, \\ \dot{\theta} &= 1 + \frac{\varepsilon}{r} \left\langle A \begin{pmatrix} u \\ v \end{pmatrix}, \begin{pmatrix} -\sin\theta \\ \cos\theta \end{pmatrix} \right\rangle. \end{aligned}$$

Perform a rescaling in ε by putting $r = \varepsilon^{1/3}\bar{r}$ and $\lambda = \varepsilon^{2/3}\bar{\lambda}$. This brings

$$\begin{aligned} \dot{\bar{r}} &= \varepsilon^{2/3} \left[\bar{\lambda}\bar{r} - \bar{r}^3 + \varepsilon^{1/3}\mathcal{O}(\bar{r}^4) + \left\langle A \begin{pmatrix} u \\ v \end{pmatrix}, \begin{pmatrix} \cos\theta \\ \sin\theta \end{pmatrix} \right\rangle \right], \\ \dot{\theta} &= \varepsilon^{2/3} \left[\varepsilon^{-2/3} + \frac{1}{\bar{r}} \left\langle A \begin{pmatrix} u \\ v \end{pmatrix}, \begin{pmatrix} -\sin\theta \\ \cos\theta \end{pmatrix} \right\rangle \right], \end{aligned} \tag{8}$$

were $A = A_0(\lambda) + \varepsilon^{1/3}\mathcal{O}(\bar{r})$. Multiplying by a factor $\varepsilon^{-2/3}$ and taking the limit $\varepsilon \downarrow 0$ gives

$$\dot{\bar{r}} = \bar{\lambda}\bar{r} - \bar{r}^3 + \langle A(u, v), (\cos\theta, \sin\theta) \rangle$$

for the radial component.

Noting that (u, v) lies in a unit disk, $A(u, v)$ lies in an ellipse. If we let a and b be the major and minor axes of this ellipse, then by a rotation of coordinates we may transform the last equation into

$$\dot{\bar{r}} = \bar{\lambda}\bar{r} - \bar{r}^3 + au\cos\theta + bv\sin\theta. \tag{9}$$

In [11] the authors showed that the boundary of an MFI set consists of solutions of the extremal vector fields defined by the bounded noise differential equations. Observe that for $\varepsilon = 0$, (8) reads $\dot{\theta} = 1$ and $\dot{\bar{r}} = 0$ and its right hand varies continuously with ε. Hence for ε small, the $\bar{r}$ components of the extremal vector fields are approximately the extremal values of the $\bar{r}$ component. A simple calculation shows that the extremal values of the last two terms in (9) are given by:

$$\pm\sqrt{a^2\cos^2\theta + b^2\sin^2\theta}.$$

Thus the boundaries of all solutions of (9) are given by the solution $r_\pm$ of the equations:

$$\dot{r}_\pm = \bar{\lambda}r_\pm - r_\pm^3 \pm \sqrt{a^2\cos^2\theta + b^2\sin^2\theta}. \tag{10}$$

Now note that $\dot{\theta}$ is of order $\varepsilon^{-2/3}$. This allows us to average equations (10) to obtain the averaged equations:

$$\dot{\bar{r}}_\pm = \bar{\lambda}\bar{r}_\pm - \bar{r}_\pm^3 \pm \int_0^{2\pi} \sqrt{a^2\cos^2\theta + b^2\sin^2\theta}\, d\theta. \tag{11}$$

Note that the integral may be transformed into:

$$4a\int_0^{\pi/2} \sqrt{1 - \left(1 - \frac{a^2}{b^2}\right)\sin^2\theta}\, d\theta = 4aE\left(\sqrt{1 - a^2/b^2}\right),$$

where $E(k) \equiv \int_0^{\pi/2} \sqrt{1 - k^2\sin^2\theta}\, d\theta$ is the complete elliptic integral of the second kind. Thus the averaged equations for $r_\pm$ are simply:

$$\dot{\bar{r}}_\pm = \bar{\lambda}\bar{r}_\pm - \bar{r}_\pm^3 \pm c, \tag{12}$$

where $c = 4aE(\sqrt{1 - a^2/b^2})$.

The analysis of the MFI bifurcation is now straightforward. First consider the equation for $\bar{r}_+$. For all parameters, this has a hyperbolic attracting fixed point at the largest real solution of $r^3 - \lambda r - c = 0$. According to Theorem 4.1.1 in [8] the original equation has a hyperbolic attracting periodic orbit that passes close to the hyperbolic fixed point on a Poincaré section. This periodic orbit γ^+ encloses an MFI set. Further it is can be shown that any orbit beginning outside of γ^+ will converge to the MFI set.

Next consider the equation for $\bar{r}_-$. A saddle-node bifurcation occurs in the averaged equation when

$$\lambda_{\text{bif}} = \frac{3c^{2/3}}{4^{1/3}} \tag{13}$$

at

$$r^* = \left(\frac{c}{2}\right)^{\frac{1}{3}} \tag{14}$$

in which a stable and an unstable fixed point are formed. It follows from Theorem 4.3.1 in [8] that the Poincaré map for original equation also undergoes a saddle-node bifurcation near the one for the averaged equation. Thus a stable periodic orbit γ^- for r_- is created. The stable orbits γ^+ for r_+ and γ^- for r_- enclose an annular MFI set.

We summarize the above calculations. For $\lambda < \lambda_{\text{bif}}$ the disk region inside γ^+ is a minimal forward invariant set. For $\lambda \geq \lambda_{\text{bif}}$ the MFI set is the annular region bounded by γ^- and γ^+. Thus the MFI set changes discontinuously at λ_{bif} and so a hard bifurcation of type **B2** occurs. □

3 Random cycles

The deterministic Hopf bifurcation involves the creation of a limit cycle. In this section we comment on the occurrence of attracting random cycles.

Random cycles are defined in analogy with random fixed points [1]; for its definition we need to consider the noise realizations ξ and the flow $\Phi_\lambda^t(x,\xi)$ for two sided time $t \in \mathbb{R}$. We henceforth consider the skew product flow

$$(x,\xi) \mapsto \left(\Phi_\lambda^t(x,\xi_t), \theta^t\xi\right)$$

with

$$\theta^t\xi_s = \xi_{t+s}$$

for $t, s \in \mathbb{R}$. We formulate a result with a relaxed notion of attracting random cycle, as we allow for time reparameterizations. The notion implies though that a Poincaré return map on a section $\{\theta = 0\}$ has an attracting random fixed point.

Recall that a random fixed point is a map $R : \mathcal{U} \to \mathbb{R}^2$ that is flow invariant,

$$\Phi_\lambda^t(R(\xi),\xi) = R(\theta^t\xi)$$

for $\mathbb{P}$ almost all ξ. A random cycle is defined as a continuous map $S : \mathcal{U} \times \mathbb{S}^1 \to \mathbb{R}^2$ that gives an embedding of a circle for $\mathbb{P}$ almost all $\xi \in \mathcal{U}$ and is flow invariant in the sense

$$(S(\theta^t\xi, \mathbb{S}^1), t) \subset \bigcup_{t\in\mathbb{R}} (\Phi_\lambda^t(S(\xi,\mathbb{S}^1),\xi), t)$$

Different regularities of the embeddings $\mathbb{S}^1 \mapsto S(\xi,\mathbb{S}^1)$ may be considered.

The following result establishes the occurrence of attracting random cycles following the hard bifurcation, for small noise amplitudes. We confine ourselves with a statement on continuous random cycles, thus avoiding for instance constructions of invariant cone fields to prove Lipschitz continuity.

Theorem 3.1. *For values of (λ, ε) with $\lambda > \lambda_{\text{bif}}$ and ε small, the MFI E_λ is diffeomorphic to an annulus and the flow Φ_λ^t admits a random cycle $S : \mathcal{U} \times \mathbb{S}^1 \to \mathbb{R}^2$ inside E_λ.*

The random cycle is attracting in the sense that there is a neighborhood U_λ of the MFI E_λ, so that for all $x \in U_\lambda$, the distance between $(\Phi_\lambda^t(x), t)$ and $\bigcup_{t\in\mathbb{R}}(S(\theta^t\xi, \mathbb{S}^1), t)$ goes to zero as $t \to \infty$.

Proof. Recall from the proof of Theorem 2.1 the blow-up differential equations in polar coordinates:

$$\begin{aligned}
\dot{\bar{r}} &= \bar{\lambda}\bar{r} - \bar{r}^3 + \varepsilon^{1/3}\mathcal{O}(\bar{r}) + \left\langle A \begin{pmatrix} u \\ v \end{pmatrix}, \begin{pmatrix} \cos\theta \\ \sin\theta \end{pmatrix} \right\rangle, \\
\dot{\theta} &= \varepsilon^{-2/3} + \frac{1}{\bar{r}} \left\langle A \begin{pmatrix} u \\ v \end{pmatrix}, \begin{pmatrix} -\sin\theta \\ \cos\theta \end{pmatrix} \right\rangle, \\
\dot{t} &= 1.
\end{aligned} \tag{15}$$

where u, v are noise realizations.

Consider a reparameterization of time, $\tau = g(\bar{r}, \theta, u, v)t$ with

$$g(\bar{r}, \theta, u, v) = 1 + \varepsilon^{2/3}\frac{t}{\bar{r}} \left\langle A \begin{pmatrix} u \\ v \end{pmatrix}, \begin{pmatrix} -\sin\theta \\ \cos\theta \end{pmatrix} \right\rangle.$$

Note that g is close to 1, in particular positive, for small values of ε. The reparameterization yields differential equations, for functions $\bar{r}, \theta, t$ of τ,

$$\begin{aligned}
\bar{r}' &= \frac{1}{g(\bar{r}, \theta, u, v)} \left(\bar{\lambda}\bar{r} - \bar{r}^3 + \varepsilon^{1/3}\mathcal{O}(\bar{r}) + \left\langle A \begin{pmatrix} u \\ v \end{pmatrix}, \begin{pmatrix} \cos\theta \\ \sin\theta \end{pmatrix} \right\rangle \right), \\
\theta' &= \varepsilon^{-2/3}, \\
t' &= \frac{1}{g(\bar{r}, \theta, u, v)}.
\end{aligned} \tag{16}$$

Note that the time reparameterization does not preserve the flow of individual cycles $S(\xi, \mathbb{S}^1)$. However, for a fixed noise realization ξ, the graph $\bigcup_{t\in\mathbb{R}}(S(\theta^t\xi, \mathbb{S}^1), t)$ is an invariant manifold for both (15) and (16). As the time parameterization has changed only by a factor $\frac{1}{g(\bar{r},\theta,u,v)}$ that is bounded and bounded away from zero, to prove the existence of an attracting random cycle it suffices to do this for (16).

Define a graph transform Γ_λ^τ on embedded circles written as graphs $\mathcal{U} \times [0, 2\pi] \mapsto [R_-, R_+]$ for suitable $0 < R_- < R_+$. That is, Γ_λ^τ is determined through the property

$$\text{graph } \Gamma_\lambda^\tau T(\xi, \cdot) = \Psi_{\lambda,\varepsilon}^\tau \text{ graph } T(\theta^{-\tau}\xi, \cdot)$$

Pick R_-, R_+ such that, in the limit $\varepsilon = 0$, $\{R_- < r < R_+\}$ is invariant. This is possible for $\bar{\lambda} > \lambda_{\text{bif}}$; note $R_- < r_- < r_+ < R_+$. Note that $\Gamma_{\lambda,\varepsilon}^\tau$ maps $C^0([0, 2\pi], [R_-, R_+])$ into itself. We obtain $S(\xi, \cdot)$

as the limit

$$S(\xi,\cdot) = \lim_{\tau\to\infty} \Gamma_\lambda^\tau T(\xi,\cdot) \tag{17}$$

computed in the supnorm on $C^0([0,2\pi],[R_-,R_+])$.

Consider the translation $s = \bar{r} - R_-$. Then s satisfies the differential equation

$$\dot{s} = (\bar{\lambda} - 3R_-^2)s - 3R_- s^2 - s^3 + \bar{\lambda}R_- - R_-^3 + a,$$

where we abbreviated $a = \left\langle A \begin{pmatrix} u \\ v \end{pmatrix}, \begin{pmatrix} \cos\theta \\ \sin\theta \end{pmatrix} \right\rangle$. We consider the differential equation for s on $[0, R_+ - R_-]$, which is invariant by the choices of R_-, R_+. Note also that the coefficient $\bar{\lambda} - 3R_-^2$ is negative. Suppose $s_1 > s_2$ are two solutions and consider the difference $u = s_1 - s_2$. Then u satisfies

$$\dot{u} = (\bar{\lambda} - 3R_-^2 - 6R_- s_2 - 3s_2^2)u - (3R_- + 3s_2)u^2 - u^3.$$

All coefficients here are negative, implying that $u(t) \to 0$ as $t \to \infty$. This computation demonstrates the convergence in (17). Likewise for small values of ε. □

Write $\bar{r} \mapsto \Pi_\lambda(\bar{r},\xi)$ for the first return map on $\{\theta = 0\}$ of $\Phi_t(\bar{r},0,\xi)$. As a corollary of the above theorem we obtain an attracting random fixed point for Π_λ.

Corollary 3.2. *For λ and ε as in Theorem 3.1, the first return map Π_λ admits a random fixed point $R(\xi)$ inside $E_\lambda \cap \{\theta = 0\}$.*

The random fixed point is attracting in the sense that there is a neighborhood U_λ of E_λ, so that for all $x \in U_\lambda \cap \{\theta = 0\}$, $|\Pi^k(x,\xi) - \Pi^k(R(\xi))| \to 0$ as $k \to \infty$.

Proof. Just note that $\Pi_\lambda = \Psi_\lambda^{2\pi\varepsilon^{2/3}}$, defined in the proof of Theorem 3.1. □

A better notion of random attracting cycle would be without time reparameterizations;

$$\Phi_\lambda^t(S(\xi,\mathbb{S}^1)) = S(\theta^t\xi,\mathbb{S}^1).$$

This would allow a discussion of the dynamics on the random cycle, such as the possibility to find an attracting random fixed point on it, compare [2, 3].

4 Simulations of bounded noise, radially symmetric Hopf.

4.1 Radially symmetric Hopf with bounded noise

In this section we reproduce invariant measures for the radially symmetric system

$$\begin{aligned} \dot{x} &= \lambda x - y - x(x^2+y^2) + \varepsilon u, \\ \dot{y} &= x + \lambda y - y(x^2+y^2) + \varepsilon v, \end{aligned} \tag{18}$$

where $\lambda \in \mathbb{R}$ is a parameter and u and v are noise terms satisfying: $u^2 + v^2 \leq 1$, representing radially symmetric noise. In the simulations below we generate the noise by stochastic differential equations with reflective boundary conditions.

For $\varepsilon = 0$ the differential equations (18) undergo a supercritical Hopf-Andronov bifurcation at $\lambda = 0$. For $\lambda < 0$ the origin is a stable global attractor. For $\lambda > 0$ the origin is unstable, but there is a circular globally attracting periodic orbit at $r = \sqrt{\lambda}$. Changing to polar coordinates we find:

$$\begin{aligned} \dot{r} &= \lambda r - r^3 + \varepsilon\alpha, \\ \dot{\theta} &= 1 + \frac{\varepsilon}{r}\beta, \end{aligned} \tag{19}$$

where

$$\alpha = (u\cos\theta + v\sin\theta) = \langle u, v\rangle \cdot \langle \cos\theta, \sin\theta\rangle$$

and

$$\beta = (-u\sin\theta + v\cos\theta) = \langle v, -u\rangle \cdot \langle \cos\theta, \sin\theta\rangle.$$

Figure 1 indicates boundaries of radial components of the MFI set for (19). Following the proof of Theorem 2.1 the boundaries of the MFI set are given by zeros of the upper and lower radial differential equations

$$\dot{r}_\pm = \lambda r_\pm - r_\pm^3 \pm \varepsilon. \tag{20}$$

From (13) and (14),

$$\lambda_{\text{bif}} = \frac{3\varepsilon^{2/3}}{4^{1/3}}, \qquad r^* = \left(\frac{\varepsilon}{2}\right)^{\frac{1}{3}}.$$

Write ρ^+ for the positive zero of the upper differential equation for r_+. For $\lambda \geq \lambda_{\text{bif}}$, let ρ_- be the largest positive zero of the lower differential equation for r_-. For $\lambda < \lambda_{\text{bif}}$ the MFI set is a disk of radius ρ_+. For $\lambda \geq \lambda_{\text{bif}}$ the MFI set is an annulus bounded by circles with radii ρ_-, ρ_+. See Figure 1.

In addition to the MFI set, another important dynamical feature of these equations is the set of equilibrium points. For $\lambda \leq 0$ these equilibrium points are stable, but for $\lambda > 0$ they are unstable.

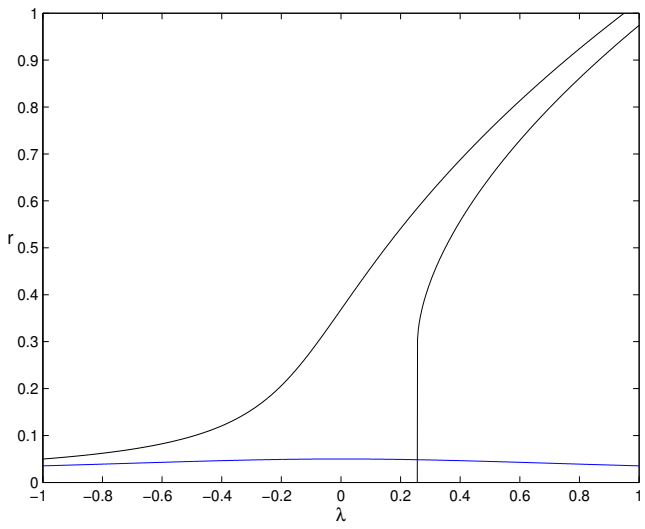

Figure 1: Boundaries of the radial components of the minimal invariant set in the random symmetric Hopf bifurcation (18). Here $\varepsilon = 0.05$. The hard bifurcation takes place at $\lambda_{\text{bif}} \approx 0.2565$ and the inner boundary has initial radius $r^* \approx 0.2924$. The MFI set changes from a disk with radius ρ_+ for $\lambda < \lambda_{\text{bif}}$ to an annulus with radii $\rho_- < \rho_+$ for $\lambda \geq \lambda_{\text{bif}}$. The graph labeled r_s indicates the boundary of the set of fixed points which are stable for $\lambda \leq 0$ and unstable for $\lambda > 0$.

These are the points that are fixed points of (18) when (u, v) is a fixed value. One can find that this set is a disk centered at the origin with radius r_s which is a solution of:

$$(1 - 2\lambda)r^6 + (1 + \lambda^2)r^2 - \varepsilon^2 = 0.$$

The radius r_s as function of λ is plotted in Figure 1.

4.2 Simulations

In this section we simulate the bounded noise bifurcation for the sake of demonstration. We note that associated with MFI sets are invariant densities whose supports are the MFI sets [10]. In the symmetric Hopf bifurcation as in the previous subsection, we approximate these invariant densities for different values of λ as λ moves through the random bifurcation.

The generation of bounded noise is somewhat arbitrary without specific knowledge about the noise involved in a particular setting. In this work we generate the noise terms u and v via the stochastic system:

$$\begin{aligned} du &= \sigma \, dW_1, \\ dv &= \sigma \, dW_2, \end{aligned} \tag{21}$$

where dW_1 and dW_2 are independent (of each other) normalized white noise processes and (21) are interpreted in the usual way as Itō integral equations. In order to assure boundedness and radial symmetry, we restrict (u, v) to the unit disk and impose reflective boundary conditions. Other methods of generating and bounded the noise did not produce significantly difference in the results.

The parameter σ can be interpreted as the rapidity of the noise. If σ is small, then u and v change slowly and as σ increases, they change more quickly. It turns out in our simulations using this noise that the value of σ has a strong influence on the characteristics of the invariant density of (18).

In the first set of simulations Figure 2, $\sigma = 1.0$ as an example of fast noise and in Figure 3, $\sigma = 0.00001$ to show slow noise. Note that for slow noise and $\lambda > 0$ there is a separation of time scales. Specifically, for each λ and each set of values of (u, v) the deterministic system defined by holding (u, v) fixed has an exponentially attracting periodic orbit. We expect then that the invariant density is concentrated on the set which is the union of all of these deterministic limit cycles. For fast noise, this will not be the case and as is observed in Figure 2, the approximated invariant densities tend to be smoother than for slow noise.

In both sets of simulations we use $\varepsilon = .1$. This leads to the following values of the bifurcation parameter and the radius of the inner boundary of the MFI set at the bifurcation:

$$\lambda_{\text{bif}} = \frac{3\varepsilon^{2/3}}{4^{1/3}} = 0.407163, \qquad r^* = \left(\frac{\varepsilon}{2}\right)^{\frac{1}{3}} = 0.368403.$$

We began the simulations by selecting random initial values for (u, v) and (x, y). As we did not need an accurate solution to generate the noise we approximated solutions to the SDE in (21) using a first order Taylor method, namely Euler's method. We then added this noise into the system in (18), which we solved using a second order Adam's-Bashforth method.

After selecting the initial noise term and a starting point for the RDE, we ran the system for 1000 iterations to allow the solution to the RDE to move into the MFI sets. We then ran the system for 5×10^5 iterations and recorded the values of every fifth (x, y) coordinate. We repeated this process for 10^2 starting points and recorded a total of 10^7 points, which we used to generate a 2-dimensional histogram. Bright regions indicate that large numbers of samples were observed in this region indicating a higher value of the invariant density. Darker regions indicate lower density.

The deterministic bifurcation takes place at $\lambda = 0$ and the random bifurcation occurs at $\lambda_{\text{bif}} \approx 0.4072$. In each set of figures, the densities are plotted for multiples of λ_{bif}; namely for $\lambda = .01\,\lambda_{\text{bif}}, .05\,\lambda_{\text{bif}}, .1\,\lambda_{\text{bif}}, .5\,\lambda_{\text{bif}}, \lambda_{\text{bif}}$, and, $1.1\,\lambda_{\text{bif}}$. The outer circle is the outer boundary of the MFI set, the circle inside the MFI is the stable periodic orbit of the deterministic system and the inner circle that appears at λ_{bif} is the inner boundary of the MFI set. It has initial radius $r^* = 0.3684$.

The invariant densities are positive for points inside the MFI set, but can be expected to go to zero very rapidly as the boundary is approached, compare [15]. Also note that the densities become undetectably small in the center long before the random bifurcation.

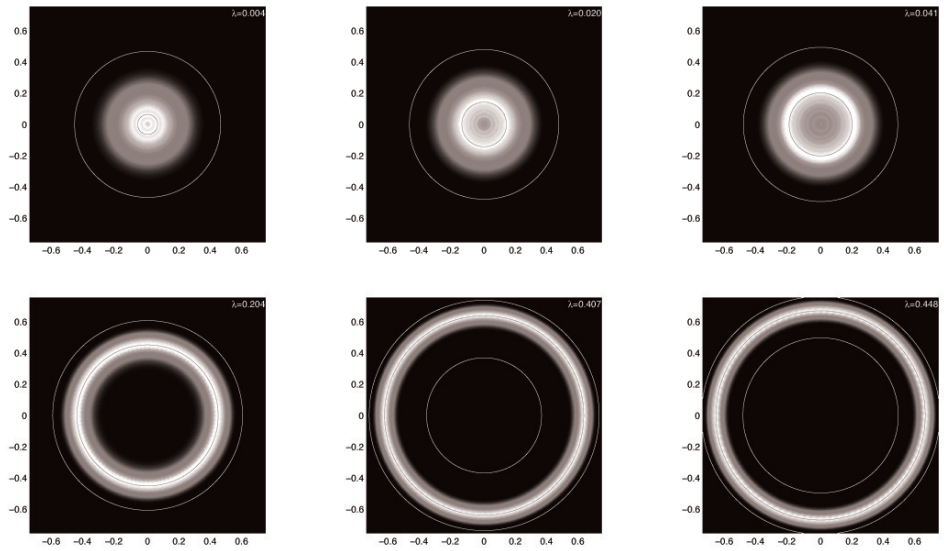

Figure 2: Images of the invariant densities for fast noise. Here $\sigma = 1$ and $\varepsilon = 0.1$.

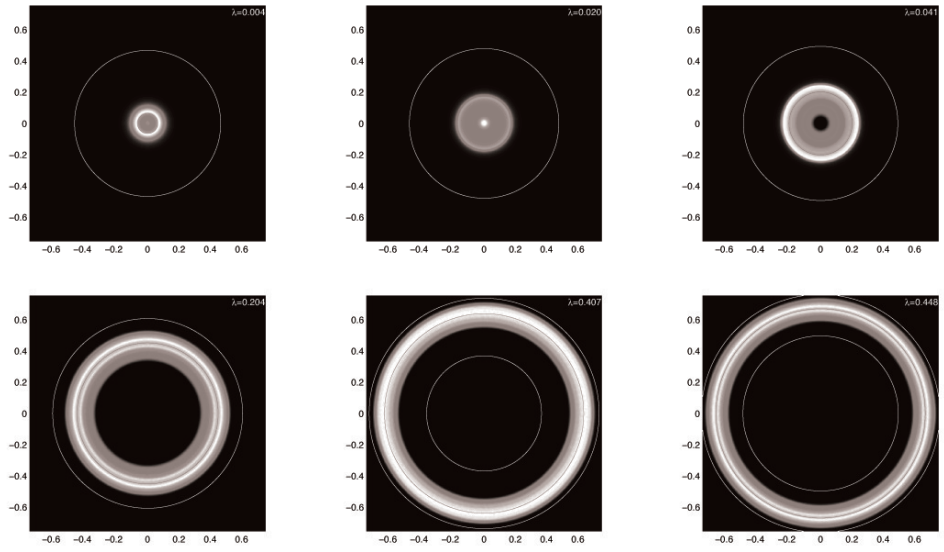

Figure 3: Images of the invariant densities for slow noise. Here $\sigma = .00001$ and $\varepsilon = 0.1$.

A movie of the simulations can be found at http://www.youtube.com/watch?v=4tVtWGdVMi8.

Acknowledgement

T.Y. was partially supported by NIH-NIGMS grant R01GM090207.

References

[1] L. Arnold, *Random Dynamical Systems*, Springer Monographs in Mathematics. Springer-Verlag, Berlin, 1998.

[2] L. Arnold, G. Bleckert, K. R. Schenk-Hoppé, The stochastic Brusselator: parametric noise destroys Hopf bifurcation, Stochastic dynamics (Bremen, 1997), 71–92, Springer, New York, 1999.

[3] L. Arnold, N. Sri Namachchivaya, K. R. Schenk-Hoppé, Towards an understanding of stochastic Hopf bifurcation: a case study, *Internat. J. Bifur. Chaos Appl. Sci. Angrg* **6** (1996), 1947–1975.

[4] I. Bashkirtseva, L. Ryashko, H. Schurz, Analysis of noise-induced transitions for Hopf system with additive and multiplicative random disturbances, *Chaos Solitons Fractals* **39** (2009), 72–82.

[5] F. Colonius, W. Kliemann, Topological, smooth and control techniques for perturbed systems, in *Stochastic Dynamic*, eds. H. Crauel and M. Gundlach, Springer-Verlag, New York, 1999.

[6] F. Colonius, W. Kliemann, *The dynamics of control* with an appendix by Lars Grace. Systems & Control: Foundations & Applications. Birkhauser Boston, Inc., Boston, MA, 2000.

[7] J.L. Doob, *Stochastic Processes*, Wiley, New York, 1953.

[8] J. Guckenheimer and P. Holmes, *Nonlinear Oscillations, Dynamical Systems, and Bifurcations of Vector Fields*, Springer-Verlag, New York, AMS **42**, 1983.

[9] F. Hoppensteadt and E. Izhikevich, *Weakly connected Neural Networks*, Springer-Verlag, New York, AMS **126**, 1997.

[10] A.J. Homburg and T. Young, Hard bifurcations in dynamical systems with bounded random perturbations, *Regular & Chaotic Dynamics* **11** (2006), 247–258.

[11] A.J. Homburg and T. Young, Bifurcations for Random Differential Equations with Bounded Noise on Surfaces. *Topol. Methods Nonlinear Anal.* 35 (2010), 77–98

[12] R.A. Johnson, Some questions in random dynamical systems involving real noise processes, in *Stochastic Dynamic*, eds. H. Crauel and M. Gundlach, Springer-Verlag, New York, 1999.

[13] Yu. A. Kuznetsov, *Elements of applied bifurcation theory*, Springer Verlag, 1995.

[14] S. Wieczorek Stochastic bifurcation in noise-driven lasers and Hopf oscillators. *Phys. Rev. E* **79** (2009), 036209, 10 pp.

[15] H. Zmarrou and A.J. Homburg, Bifurcations of stationary densities of random diffeomorphisms, *Ergod. Th. Dyn. Systems* **27** (2007), 1651–1692.